JACS
JOURNAL OF THE AMERICAN CHEMICAL SOCIETY
Communication
pubs.acs.org/JACS

Influence of Anions in Silver Supramolecular Frameworks: Structural Characteristics and Sorption Properties.

Irene Bassanetti,[†] Francesco Mezzadri,[†] Angiolina Comotti,[§] Piero Sozzani,[§] Marcello Gennari,[†,‡] Gianluca Calestani,[†] and Luciano Marchiò*[,†]

[†]Dipartimento di Chimica Generale ed Inorganica, Chimica Analitica, Chimica Fisica, Parco area delle Scienze 17/a, Università degli Studi di Parma, Parma, Italy

[§]Department of Materials Science, University of Milano Bicocca, Via R. Cozzi 53, 20125 Milano, Italy

Supporting Information

ABSTRACT: The complexation of a preorganized thioether-functionalized bis(pyrazolyl)methane ligand (L) with silver precursors produces supramolecular structures organized at two hierarchical levels: $[AgL]_6(X)_6$ metal–organic cyclic hexamers and their organization in 3D architectures. The cyclic toroidal hexamers of 22–26 Å external diameter are found to be stable already in solution before self-assembly into the crystalline state. In the 3D lattice, the hexameric building block are arranged in different highly symmetric space groups as a function of a variety of anions (cubic $Fd\bar{3}$ with PF_6^- or BF_4^- and rhombohedral $R\bar{3}$ with $CF_3SO_3^-$ or NO_3^-) and form cavities with the geometrical shapes of Platonic solids (tetrahedron and octahedron) that can be occupied by a variety of solvent molecules. Upon evacuation, cubic crystals can produce stable frameworks with permanent porosity, which can absorb reversibly several vapors, CO_2 and CH_4.

Coordination-driven self-assembly of metals and properly designed molecular linkers leads to the formation of discrete supramolecules of particular geometrical shapes (polygons and polyhedra).[1,2] These supramolecules can in turn self-assemble into a variety of complex crystalline architectures enabling the exploration of a new fertile field to produce porous materials.[3−6] The weak interactions ($\pi-\pi$, CH$-\pi$, H-bonds, van der Waals) that shape organic supramolecular materials[7−9] can be complemented by more directionally and spatially oriented coordination bonds. The judicious choice of metal centers and ligand types (rigidity/flexibility and donor atom set) can enhance the probability of obtaining the desired structural topologies of metal-containing frameworks.[1,10−13] Among the many and structurally diverse ligands used as building blocks in supramolecular architectures, opportunely functionalized bis(pyrazolyl)methane fragments can be preorganized to control and possibly predict the metal–organic spatial arrangement.[14−20] Given the neutral nature of many ligands, a metal-based supramolecular moiety usually necessitates the inclusion of anions as charge-balance components, which can in turn exert a significant influence on the supramolecular organization, nucleation, and in the resulting network topology.[21−23]

In this paper, we present the preparation of Ag(I)/Cu(I)-bis(pyrazolyl)methane hexameric toroidal supramolecules that self-assemble, at a higher hierarchical level, into a diversity of 3D supramolecular architectures and cavities as function of the anion used. The counterions (BF_4^-, PF_6^-, NO_3^-, and $CF_3SO_3^-$) largely modulate the structure of the toroidal hexamers and have a profound impact on the crystal framework arrangement. Moreover, we show that the AgL-B and AgL-P (L = ligand, B = BF_4^-, P = PF_6^-) compounds are structurally stable to solvent desorption and that the formation of crystals with permanent porosity is promoted, as demonstrated by vapor and gas absorption measurements. The self-assembled toroidal hexamers were synthesized with a ditopic N_2S donor ligand, which is derived from a thioether-functionalized bis(pyrazolyl)methane moiety and which coordinates favorably with Ag(I)/Cu(I). The preferred conformation of the ligand[20,24] and the consequent orientation of the N_2 and S promotes the persistence of hexameric supramolecular structures. In AgL-B compound, the hexamer has the shape of a torus measuring 26 Å in diameter, with a central hydrophobic pore of 5.1 Å (Figure 1).

The compound crystallizes in the cubic space group $Fd\bar{3}$, and the crystal packing is determined by BF_4^-, which interposes between two silver atoms belonging to two adjacent hexamers. The centroids of four hexamers occupy the vertex of a tetrahedron, thus, defining a tetrahedral cavity bordered by phenyl rings (Figure 2, intracapsular space highlighted in green with an approximate cavity diameter of 6 Å). The packing of the spheres forms a system of interconnecting cavities lined with pyrazole methyls (intercapsular space highlighted in yellow with an approximate cavity diameter of 7 Å). Isostructural crystals could be obtained by crystallizing AgL-B in different solvents such as THF/hexanes, CH_2Cl_2/hexanes, and acetone/diethyl-ether. Because Ag(I) and Cu(I) have similar geometric preferences, a similar molecular structure is obtained when Cu(I) is used in place of Ag(I), the major difference being the metal-donor atom bond lengths. For CuL-B, these bond lengths are on average 0.2 Å shorter than those in AgL-B. The replacement of Ag(I) with Cu(I) does, however, have a minimal effect on the size of the internal cross section of

Received: April 24, 2012
Published: May 22, 2012

dx.doi.org/10.1021/ja303940d | J. Am. Chem. Soc. 2012, 134, 9142–9145

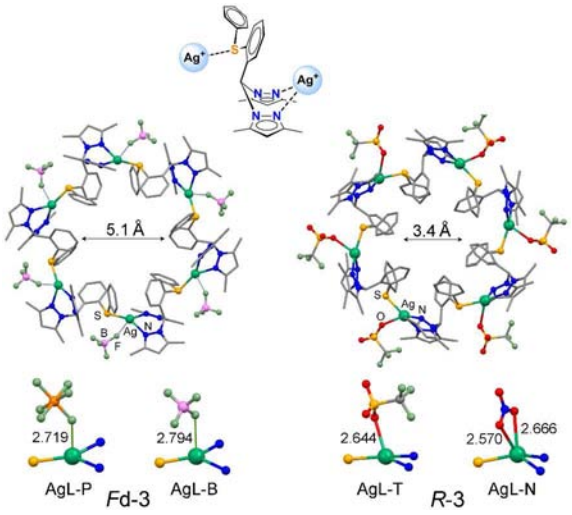

Figure 1. Above, ligand structure. Middle, toroidal shape of the hexamers of AgL-B/AgL-P and AgL-T/AgL-N as derived by single-crystal X-ray diffraction. Below, coordination environments at the metal centers.

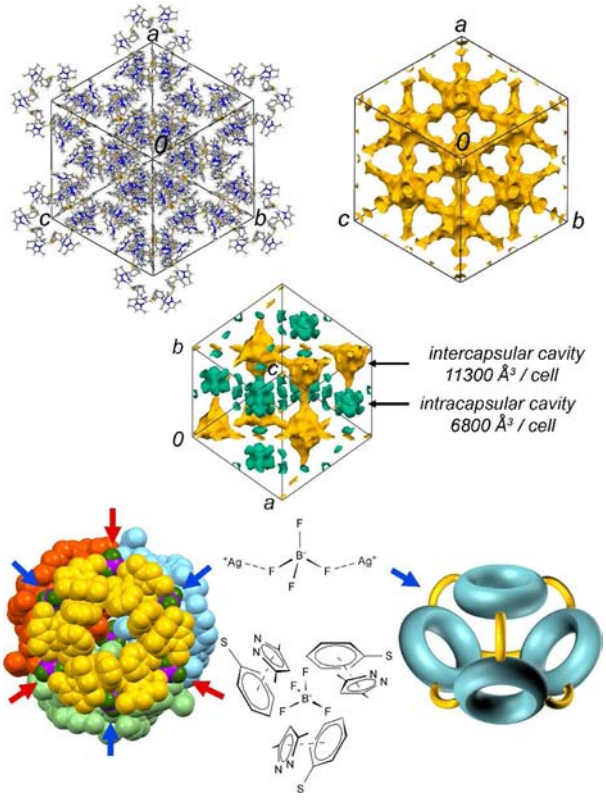

Figure 2. Above, crystal packing of AgL-B depicting the rigid part of the structure in stick and the cavities in yellow. Middle, the two different types of cavities are depicted in yellow and green, respectively. Below, description of the supramolecular contacts between the BF_4^- anions and the hexameric moieties.

the hexameric toroid; in the copper complex, this distance is 5.0 Å (Figure S1).

Because BF_4^- anions connect the hexameric supramolecules to create the 3D overall crystal framework, we expect that the counterion plays a significant role in the construction of the crystal lattice. Thus, we synthesized different silver complexes by using different counterions: PF_6^-, NO_3^-, and $CF_3SO_3^-$. In all cases, a positively charged cyclic hexamer is generated. The highly symmetric PF_6^- anion has the same influence over the entire structure as BF_4^- (Figure S1). In fact, the two complexes are isostructural, with the phosphorus atom occupying the same sites as the boron atoms; the only difference between the two complexes is the localization of the fluorine atoms. This difference is most likely due to the high symmetry and shapes of BF_4^- and PF_6^-, allowing both of these ions to fit within the same spherical site. A remarkable difference is observed in the crystal structures formed by the NO_3^- and $CF_3SO_3^-$ anions (AgL-N and AgL-T, respectively) with respect to the AgL-B and AgL-P compounds: (i) the hexameric molecular torus has a smaller diameter of 22 Å, and the cross section of the internal pore is decreased to 3.4 Å; (ii) the interaction between the counterion and the silver ions is distinct; in AgL-N, the nitrate acts as an O_2 bidentate ligand, whereas in AgL-T, the triflate is monodentate (Figure 1 and Figure S1); (iii) the compounds crystallize in the rhombohedral space group $R\bar{3}$ and the crystal packing shows the presence of octahedral cavities formed by six hexameric units (approximate diameter = 7.6 Å). The octahedral cavity is in communication with symmetry-related cavities aligned along the C3 crystallographic axis by means of a hydrophobic window. Notably, the volumes of the cavities amount to 40% and 36% of the unit cell volumes of the AgL-N and AgL-T compounds, respectively, whereas in the AgL-B and AgL-P compounds, the volumes account for 27% of the unit cell volume. Only the solvent guest molecules of AgL-T could be located within the cavities. Specifically, part of a hexane molecule is located inside the hydrophobic window, and part extends outside of the window toward the center of the cavity occupied by THF molecules (Figure 3).

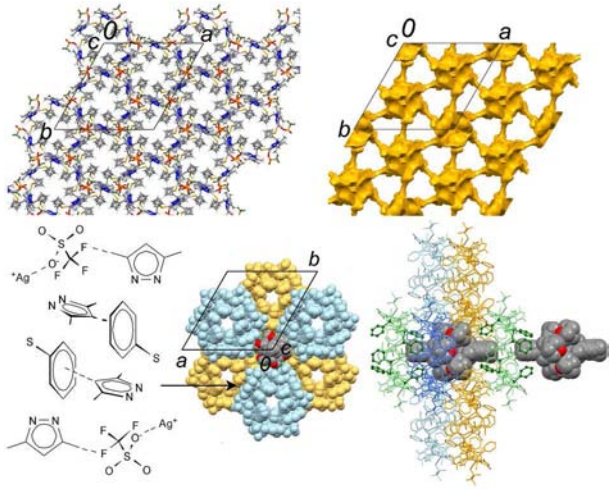

Figure 3. Above, crystal packing of AgL-T depicting the rigid part of the structure in stick and the cavities in yellow. Below, description of the supramolecular contacts between the triflate anions and the hexameric moieties. Disordered solvent molecules are shown in Spacefill mode (gray and red).

The reason for the attainment of these two classes of compounds, AgL-B/AgL-P and AgL-T/AgL-N, as function of anions is to be found in the formation of hexameric macrocycles already in solution. In fact, this has been demonstrated by ESI−MS spectrometry (Figure S4) and by pulsed-gradient spin−echo (PGSE) NMR measurements which provide information about the hydrodynamic radii (r_H) of

dx.doi.org/10.1021/ja303940d | J. Am. Chem. Soc. 2012, 134, 9142−9145

species in solution. These latter experiments were performed in CD_2Cl_2 (ε= 9.1) and in acetone-d^6 (ε = 20.7) at three different concentrations (0.1−0.001 M), because the aggregation process and the ion pairing depend on the solvent polarities[25] (Figures S5−S7). The measured r_H radii for AgL-B and AgL-T are in the 6.4(2)−7.6(3) A and 6.2(2)−6.7(3) Å ranges, respectively. These values are in agreement with the 7.8 and 6.4 Å mean values of radii, as derived from single-crystal X-ray structures (Tables S3 and S4). The r_H values are consistent with the presence of isolated hexameric units in solution, at least in the investigated concentration interval, suggesting that the robust supramolecules pre-exist to the crystallization process.

The powder X-ray diffraction patterns demonstrate that the crystals of AgL-B/AgL-P retain a long-range structural order up to 180 °C, as also confirmed by calorimetric analysis (Figures S8−S14). The compounds subjected to evacuation from solvents at 10^{-3} mmHg and 110 °C overnight exhibited substantially unaltered powder patterns with small reductions in the unit cell parameters, suggesting the formation of porous crystalline materials (Figure 4). Solid-state NMR spectra

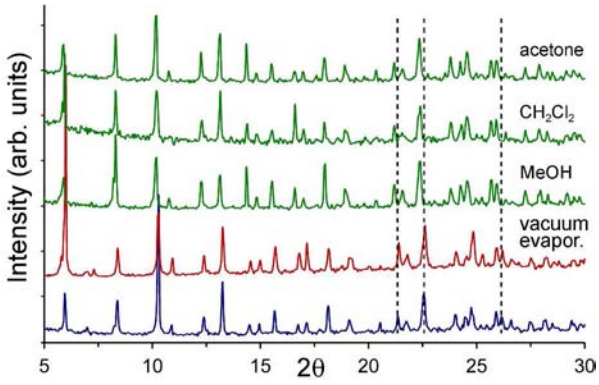

Figure 4. Effect of the solvent absorption on AgL-B crystals. Freshly ground crystals, blue. Crystals subjected to high vacuum and T = 100 °C for 2 h, red. The evacuated crystals were then exposed to saturated solvent vapors (methanol, dichlorometane, or acetone), green.

confirm the absence of solvent molecules in the crystal materials (Figure S15). When the evacuated crystalline materials are placed in a chamber saturated with solvent vapor, the resulting powder patterns show a 2.7−3.7% increase in the unit cell volume depending on the solvent employed. These data may be interpreted as an enlargement of the unit cell parameters taking place to accommodate the solvent molecules within the empty cavities.[26] This behavior is observed using dichloromethane, acetone, and methanol, and several cycles of vacuum followed by exposure to solvent vapor can be applied to the compounds without the loss of structural order (Figures S12 and S13). The opposite behavior is exhibited by the crystals of AgL-T/AgL-N: these compounds lose their crystallinity when subjected to vacuum treatment (Figures S10 and S11) and do not regain it after exposure to solvent vapor.[27−29] This behavior is most likely the result of the different supramolecular arrangements and crystal packing. In fact, a considerable contribution to the stabilization of the 3D porous structure of AgL-B/AgL-P is made by the anions that connect adjacent hexameric toroids through moderately strong Ag−F interactions. In contrast, in AgL-T/AgL-N crystals, the toroids are held together by weaker CH···π/CH···F and CH···S/CH···O interactions (see Figure S2).

The permanent porosity of the AgL-B/AgL-P compounds was demonstrated by adsorption isotherms of gases. AgL-B can absorb 76 cm^3(STP)/g of CO_2 at 195 K and 1 atm (15.1 wt %), whereas 22 cm^3/g of methane was adsorbed under the same pressure and temperature conditions (Figure 5). The measured

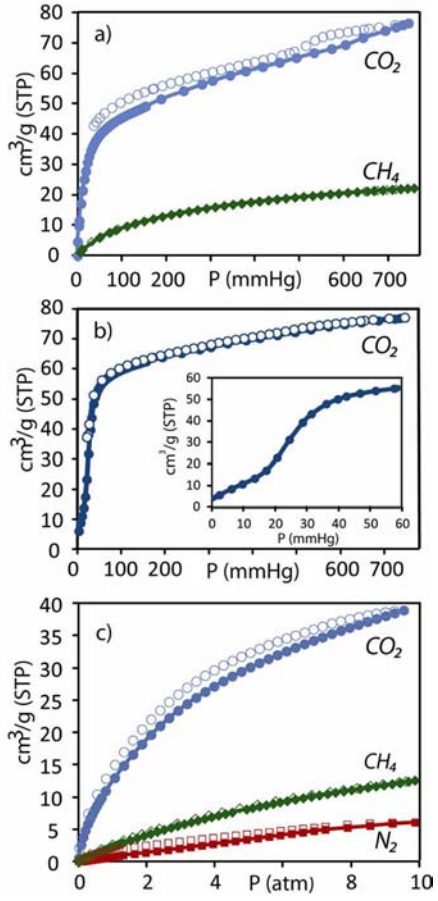

Figure 5. (a) Adsorption/desorption isotherms for CO_2 and CH_4 onto porous AgL-B at 195 K. (b) CO_2 adsorption/desorption isotherm for the porous AgL-P compound at 195 K. Inset, enlargement of the low pressure region. (c) Adsorption/desorption isotherms for CO_2, CH_4 and N_2 onto AgL-B at room temperature and up to 10 atm.

CO_2 capacity, equal to 3.44 mmol/g, corresponds to an occupied volume of 9600 $Å^3$ per unit cell (dCO_2 = 1.5 g/cm^3 was used) which matches well with the open-pore capacity of the intercapsular space, 11300 $Å^3$ per unit cell, as explored with a sphere with a diameter of 3.3 Å (corresponding to the kinetic diameter of CO_2). Thus, this result indicates the virtually complete filling of the intercapsular space which is easily accessible to gas species via diffusion. In contrast, CO_2 molecules are prevented from entering the capsules by the presence of anions occupying the aperture at the center of the cyclic hexamers. In the case of AgL-P, the CO_2 adsorption isotherm at 195 K reaches the plateau value of 77 cm^3(STP)/g at 1 atm, which is comparable to the values for the isostructural BF_4^--containing compound. The adsorption isotherm does not show a Langmuir profile but exhibits a moderate initial slope followed by a neat increase at a pressure of 18 mmHg, indicating that a gate pressure is necessary to promote the openings of the pores. As far as the uptake values are concerned, these systems are more effective than Ag-based imidazolate frameworks containing cyclic coordination struc-

dx.doi.org/10.1021/ja303940d | J. Am. Chem. Soc. 2012, 134, 9142−9145

tures recently described.[13] Furthermore, the porous materials selectively adsorb CO_2 over CH_4 and N_2 at room temperature and up to 10 atm, for example, AgL-B adsorbs 40 cm^3(STP)/g of CO_2 versus 12 and 6 cm^3(STP)/g of CH_4 and N_2, respectively.

At room temperature, CO_2/CH_4 selectivity is comparable or exceeds the values of most ZIFs while CO_2/N_2 selectivity is lower than several MOFs but exceeds the performance of the well-described MOF-5.[30,31] From the adsorption measurements at different temperatures, the isosteric heat of absorption was estimated to be 25 kJ/mol for CO_2 and 19 kJ/mol for CH_4, in agreement with the hydrophobic nature of the pyrazole methyl groups lining the intercapsular cavity. Indeed, these values are consistent with those measured, for instance, in methylimidazolate framework ZIF-8 and hydrophobic molecular zeolites.[32,33]

In conclusion, we reported the formation of unprecedented cyclic hexameric structures of Ag(I) or Cu(I) coordinated with properly designed multipodal bis(pyrazolyl)methane moiety functionalized with an aryl thioether group. The use of a diversity of anions results in the arrangement of the hexamers in two types of microporous 3D structures. The robustness of the crystalline structures obtained with the silver and copper ions and the BF_4^-/PF_6^- anions, which behave as connectors between hexameric supramolecules, leads to permanently porous materials that are able to reversibly entrap vapors and gases. The ability to play with two hierarchical levels of supramolecular organization—the metal–organic cyclic hexamers and the self-assembly of hexamers into capsules with the aid of anions—enabled the construction of complex architectures endowed with cavities of Platonic solid geometries (tetrahedron and octahedron). These complexes open up new perspectives for the use of cyclic metal–organic supramolecules as building blocks to fabricate innovative porous materials.

■ ASSOCIATED CONTENT

Ⓢ Supporting Information

Synthesis of the ligands and complexes, single crystal X-ray structures (CCDC 871753–871757), ESI–MS spectra, ^{1}H NMR PGSE experimental details, powder XRD experiments, thermal analyses, solid-state NMR, and gas absorption measurements. This material is available free of charge via the Internet at http://pubs.acs.org.

■ AUTHOR INFORMATION

Corresponding Author

marchio@unipr.it

Present Address

‡Université Joseph Fourier Grenoble 1/CNRS, Département de Chimie Moléculaire, UMR-5250, 38041 Grenoble Cedex 9 France.

Notes

The authors declare no competing financial interest.

■ ACKNOWLEDGMENTS

This work was supported by the Università degli Studi di Parma. Cariplo Foundation and Regione Lombardia are acknowledged for financial support. The authors thank M. Beretta for adsorption measurements and S. Bracco and A. Cattaneo for solid-state NMR characterization.

■ REFERENCES

(1) Chakrabarty, R.; Mukherjee, P. S.; Stang, P. J. *Chem. Rev.* **2011**, *111*, 6810–6918.
(2) Dalgarno, S. J.; Power, N. P.; Atwood, J. L. *Coord. Chem. Rev.* **2008**, *252*, 825–841.
(3) Burd, S. D.; Ma, S. Q.; Perman, J. A.; Sikora, B. J.; Snurr, R. Q.; Thallapally, P. K.; Tian, J.; Wojtas, L.; Zaworotko, M. J. *J. Am. Chem. Soc.* **2012**, *134*, 3663–3666.
(4) Inokuma, Y.; Kawano, M.; Fujita, M. *Nat. Chem.* **2011**, *3*, 349–358.
(5) Marti-Rujas, J.; Islam, N.; Hashizume, D.; Izumi, F.; Fujita, M.; Kawano, M. *J. Am. Chem. Soc.* **2011**, *133*, 5853–5860.
(6) Duriska, M. B.; Neville, S. M.; Lu, J. Z.; Iremonger, S. S.; Boas, J. F.; Kepert, C. J.; Batten, S. R. *Angew. Chem., Int. Ed.* **2009**, *48*, 8919–8922.
(7) Mastalerz, M. *Angew. Chem., Int. Ed.* **2012**, *51*, 584–586.
(8) Dalgarno, S. J.; Thallapally, P. K.; Barbour, L. J.; Atwood, J. L. *Chem. Soc. Rev.* **2007**, *36*, 236–245.
(9) Sozzani, P.; Bracco, S.; Comotti, A.; Ferretti, L.; Simonutti, R. *Angew. Chem., Int. Ed.* **2005**, *44*, 1816–1820.
(10) Bunzen, J.; Iwasa, J.; Bonakdarzadeh, P.; Numata, E.; Rissanen, K.; Sato, S.; Fujita, M. *Angew. Chem., Int. Ed.* **2012**, *51*, 3161–3163.
(11) Moulton, B.; Zaworotko, M. J. *Chem. Rev.* **2001**, *101*, 1629–1658.
(12) Oliveri, C. G.; Ulmann, P. A.; Wiester, M. J.; Mirkin, C. A. *Acc. Chem. Res.* **2008**, *41*, 1618–1629.
(13) Wang, Y.; He, C. T.; Liu, Y. J.; Zhao, T. Q.; Lu, X. M.; Zhang, W. X.; Zhang, J. P.; Chen, X. M. *Inorg. Chem.* **2012**, *51*, 4772–4778.
(14) Santillan, G. A.; Carrano, C. J. *Inorg. Chem.* **2008**, *47*, 930–939.
(15) Santillan, G. A.; Carrano, C. J. *Cryst. Growth Des.* **2009**, *9*, 1590–1598.
(16) Reger, D. L.; Foley, E. A.; Smith, M. D. *Inorg. Chem.* **2010**, *49*, 234–242.
(17) Reger, D. L.; Foley, E. A.; Semenluc, R. F.; Smith, M. D. *Inorg. Chem.* **2007**, *46*, 11345–11355.
(18) Carrion, C. M.; Duràn, G.; Jalon, F. A.; Manzano, B. R.; Rodríguez, A. M. *Cryst. Growth Des.* **2012**, *12*, 1952–1969.
(19) Morin, T. J.; Merkel, A.; Lindeman, S. V.; Gardinier, J. R. *Inorg. Chem.* **2010**, *49*, 7992–8002.
(20) Bassanetti, I.; Marchiò, L. *Inorg. Chem.* **2011**, *50*, 10786–10797.
(21) Giles, I. D.; Chifotides, H. T.; Shatruk, M.; Dunbar, K. R. *Chem. Commun.* **2011**, *47*, 12604–12606.
(22) Campos-Fernandez, C. S.; Schottel, B. L.; Chifotides, H. T.; Bera, J. K.; Bacsa, J.; Koomen, J. M.; Russell, D. H.; Dunbar, K. R. *J. Am. Chem. Soc.* **2005**, *127*, 12909–12923.
(23) Halper, S. R.; Do, L.; Stork, J. R.; Cohen, S. M. *J. Am. Chem. Soc.* **2006**, *128*, 15255–15268.
(24) Gennari, M.; Bassanetti, I.; Marchiò, L. *Polyhedron* **2010**, *29*, 361–371.
(25) Macchioni, A.; Ciancaleoni, G.; Zuccaccia, C.; Zuccaccia, D. *Chem. Soc. Rev.* **2008**, *37*, 479–489.
(26) Plevert, J.; Gentz, T. M.; Laine, A.; Li, H. L.; Young, V. G.; Yaghi, O. M.; O'Keeffe, M. *J. Am. Chem. Soc.* **2001**, *123*, 12706–12707.
(27) Uemura, K.; Kitagawa, S.; Kondo, M.; Fukui, K.; Kitaura, R.; Chang, H. C.; Mizutani, T. *Chem.—Eur. J.* **2002**, *8*, 3586–3600.
(28) Uemura, K.; Kitagawa, S.; Fukui, K.; Saito, K. *J. Am. Chem. Soc.* **2004**, *126*, 3817–3828.
(29) Carlucci, L.; Ciani, G.; Moret, M.; Proserpio, D. M.; Rizzato, S. *Angew. Chem., Int. Ed.* **2000**, *39*, 1506–1510.
(30) Liu, J.; Thallapally, P. K.; McGrail, B. P.; Brown, D. R.; Liu, J. *Chem. Soc. Rev.* **2012**, *41*, 2308–2322.
(31) Liu, B.; Smit, B. *Langmuir* **2009**, *25*, 5918–5926.
(32) Huang, H. L.; Zhang, W. J.; Liu, D. H.; Liu, B.; Chen, G. J.; Zhong, C. L. *Chem. Eng. Sci.* **2011**, *66*, 6297–6305.
(33) Comotti, A.; Bracco, S.; Distefano, G.; Sozzani, P. *Chem. Commun.* **2009**, 284–286.